PNAS RESEARCH ARTICLE | PHYSICS

Experimental observation of curved light-cones in a quantum field simulator

Mohammadamin Tajik[a,1], Marek Gluza[b], Nicolas Sebe[a,c,d], Philipp Schüttelkopf[a], Federica Cataldini[a], João Sabino[a,e], Frederik Møller[a], Si-Cong Ji[a], Sebastian Erne[a], Giacomo Guarnieri[c], Spyros Sotiriadis[c,f], Jens Eisert[c,g,1], and Jörg Schmiedmayer[a]

Edited by Angel Rubio, Max-Planck-Institut fur Struktur und Dynamik der Materie, Hamburg, Germany; received January 23, 2023; accepted March 24, 2023

We investigate signal propagation in a quantum field simulator of the Klein–Gordon model realized by two strongly coupled parallel one-dimensional quasi-condensates. By measuring local phononic fields after a quench, we observe the propagation of correlations along sharp light-cone fronts. If the local atomic density is inhomogeneous, these propagation fronts are curved. For sharp edges, the propagation fronts are reflected at the system's boundaries. By extracting the space-dependent variation of the front velocity from the data, we find agreement with theoretical predictions based on curved geodesics of an inhomogeneous metric. This work extends the range of quantum simulations of nonequilibrium field dynamics in general space–time metrics.

quantum simulation | curved metrics | light-cones | ultracold atomic gases | quantum fields

Light-cones embody one of the most fundamental principles in physics: Causality. When constructing models describing fundamental interactions in nature, one of the basic requirements is the existence of light-cones. Indeed, it has been understood that they appear as a result of the relativistic invariance of quantum fields (1). Interestingly, there are several systems whose effective dynamics are relativistically invariant, and effective light-cones also play a role. Recent experiments have revealed that effective light-cones do emerge in cold atomic gases (2, 3). In order to directly observe these light-cones, several experimental challenges had to be overcome, including resolving the system at fine length-scales and measuring relevant observables that would be able to reveal them. Tackling such issues is part of a larger research endeavor on devising quantum simulators (4–7). For example, manipulation of one-dimensional tunnel-coupled gases allows the simulation of prototypical field theories (8–11) that are of foundational importance but also, e.g., capture charge transport in nanowires (12). Here, our goal is to use this quantum simulator to explore experimentally its potential to simulate dynamics in inhomogeneous or curved metrics. Similar objectives have been the focus of analogue gravity systems (13, 14) which recently have been very successful in simulating black hole (15, 16) or cosmological (17–19) processes using cold-atom systems.

In this work, we investigate the correlation propagation in an inhomogeneous one-dimensional quantum gas. We show that correlation fronts follow geodesics of the analogue acoustic metric and find the spatial dependence of the propagation velocity in agreement with the theoretical modeling. We observe ballistic propagation of correlation fronts and discuss the detailed shape, reflections at the system's boundaries, and periodic recurrences of these correlation fronts.

Significance

Analog quantum simulators of quantum field theories have recently attracted growing attention, e.g., by enabling the testing of fundamental principles of quantum information in relativistic settings using tabletop experiments. We simulate the nonequilibrium dynamics of a quantum field simulator based on two tunneling-coupled superfluids in one-dimensional traps. We realize arbitrary trapping geometries using an optical setup based on a digital micromirror device. We present detailed studies of the dynamics of correlations propagating as fronts—located on the light-cone—and explain their curvature, reflection, and recurrences through theoretical modeling based on the geodesics of the simulated geometry. Our work introduces a versatile platform and analysis for detailed studies of quantum field theories in inhomogeneous spacetime.

Quantum Field Simulation

We use two tunneling-coupled one-dimensional superfluids to simulate the inhomogeneous Gaussian field theory in $1+1$ space–time dimensions whose action for a bosonic field ϕ can be written as:

$$\mathcal{S}[\phi] \sim \int \mathrm{d}z\mathrm{d}t \sqrt{-g} K(z) \left[g^{\mu\nu} (\partial_\mu \phi)(\partial_\nu \phi) + \tfrac{1}{2} M^2 \phi^2 \right], \quad [1]$$

where M is the mass and $g = \det(g_{\mu\nu})$. The space–time interval $\mathrm{d}s$ of the metric tensor $g_{\mu\nu}$ is given by,

$$\mathrm{d}s^2 = g_{\mu\nu} \mathrm{d}x^\mu \mathrm{d}x^\nu = -v(z)^2 \mathrm{d}t^2 + \mathrm{d}z^2. \quad [2]$$

Here, in accordance with the presented experiment, we neglected an explicit time-dependence of the parameters v and K. Light-like trajectories in this metric deviate from

The authors declare no competing interest.

This article is a PNAS Direct Submission.

[1]To whom correspondence may be addressed. Email: amintajik.physics@gmail.com or jense@zedat.fu-berlin.de.

This article contains supporting information online at https://www.pnas.org/lookup/suppl/doi:10.1073/pnas.2301287120/-/DCSupplemental.

Published May 15, 2023.

straight lines according to the function $v(z)$, i.e., the local propagation speed of (massless) fluctuations (20).

Note that, due to the conformal invariance of the Laplacian in $1+1$ dimensions, the scale factor $K(z)$ cannot be absorbed into the metric by a conformal transformation and hence has to be included in the action for generality. Nevertheless, we find the propagation of correlation fronts to be dominated by the induced metric, i.e., the massless Klein–Gordon equation, and hence neglect the spatial dependence of $K(z)$ for simplicity (*SI Appendix* for details).

In our experiment, the bosonic field ϕ corresponds to the relative phase between the two superfluids, and the space-dependent speed of sound is related to the local averaged density $\rho_0(z)$ of each superfluid, through

$$v(z) = \sqrt{g_{1D}\rho_0(z)/m}, \qquad [3]$$

where m is the mass of an atom, and g_{1D} the effective interatomic interaction strength. Thus, local tuning of the density by changing the trapping potential (21), allows for modification of the key physical parameter in the simulated metric Eq. **2**.

To initiate the light-cone propagation of correlations, we perform a quench by rapidly changing the mass parameter M from an initially large value to zero in 2 ms. Such a mass quench is a paradigmatic protocol for inducing nonequilibrium dynamics of a quantum field (22). In the experiment, the mass M is related to the single atom tunneling rate between the two atomic clouds and is quenched to zero by separating the superfluids and letting them evolve independently (8, 23).

To directly observe the light-cone dynamics, we need to measure the correlations of a local observable, like the particle density or current, which are the fundamental fields in the effective hydrodynamic description. The particle current at position z is related to the spatial derivative of the phase field, $\hat{j}(z) = \rho_0(z)\hat{u}(z)$ with the fluid velocity field

$$\hat{u}(z) = (\hbar/m)\partial_z\hat{\phi}(z). \qquad [4]$$

We measure the velocity field by extracting the spatially resolved relative phase through matterwave interferometry and show that after the quench, correlations of the velocity field exhibit light-cone fronts allowing us to explore aspects of the quantum-simulated space–time geometry.

Experimental Results

In Figs. 1*A* and 2 we show the dynamics of the two-point correlation functions of the velocity field, $C_u(z,z') = \langle\hat{u}(z)\hat{u}(z')\rangle$, at different times, prequench ($t=-2$) and postquench ($t\geq 0$), for three different experimental settings: A homogeneous density with sharp edges, an inhomogeneous density also with sharp edges, and an inhomogeneous density with smoothed edges, presented in Fig. 1 from top to bottom, respectively. All density profiles $\rho_0(z)$ are shown in Fig. 1*A*.

In accordance with Eq. **2**, assuming a vanishing macroscopic background particle flow, we find the average current $\langle\hat{u}(z)\rangle = 0$ throughout the evolution. Nevertheless, nonzero correlations $C_u(z,z') \neq 0$ mean that current fluctuations are not independent between z and z': If the correlation is positive, then in individual measurements, the current fluctuations at z and z' tend to be aligned. Conversely, for negative correlation the current fluctuations point in opposite directions. Initially, for the thermal state with large M, the velocity field has only short-range correlations, with $C_u(z,z')$ consisting of autocorrelations on the

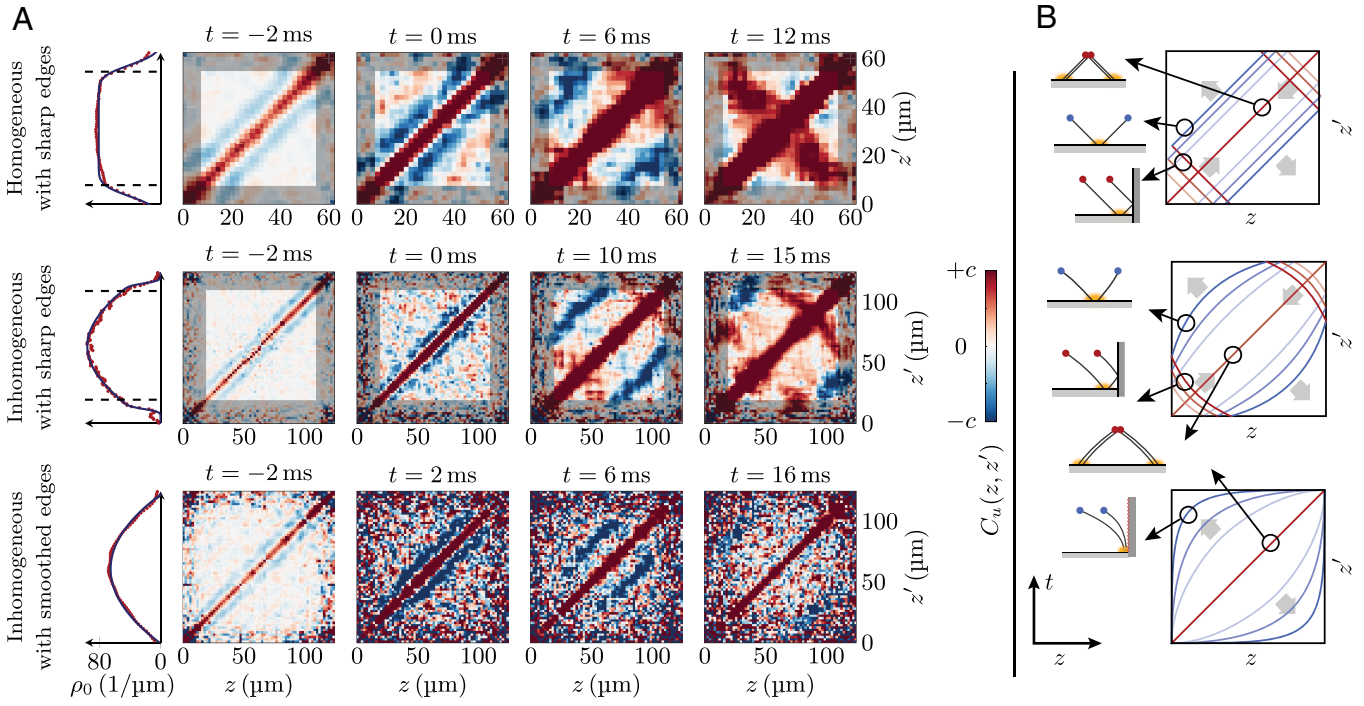

Fig. 1. Propagation of the flat and curved fronts of the two-point correlation function of the velocity field $\hat{u}$. (*A*) Measurement results of $C_u(z,z')$ at select times t, prequench ($t=-2$) and postquench ($t\geq 0$), for three experimental settings with different background density profiles as explained on the left. For each case, the measured $\rho_0(z')$ is presented by red dots, and the blue line is a fit. (*B*) Intuitive explanation of the correlation propagation fronts in different cases. At $t=0$, the points marked with the yellow dots are correlated. After the quench, evolution of correlations between these two points is traced by the light-cone trajectories of the left- and right-moving chiral fields, as depicted in the space–time sketches. The presence of narrow width fronts, as well as their shape and sign of correlations are fully explained by taking into account the effects of reflection at the boundaries and effectively curved metric. For further details, *SI Appendix*.

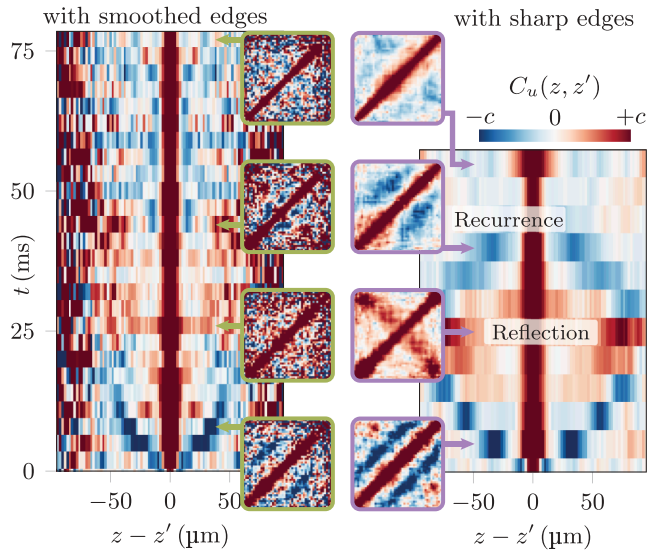

Fig. 2. Observation of light-cone propagation in the two-point correlation function of the hydrodynamic velocity field, $C_u(z,z'=-z)$, in experimental settings with (*Right*) and without (*Left*) sharp edges. In the two main plots, the antidiagonal correlations are plotted over time. For the density with sharp edges, reflection from boundaries and the recurrence is clearly observed, which is missing in the other case. For selected time steps, the full two-dimensional correlation function is plotted similar to Fig. 1.

diagonal (red) accompanied by anticorrelations (blue) parallel to the diagonal (*SI Appendix*).

After the quench, we find that the propagation of correlation fronts is determined by the geodesics of the induced space–time metric, and hence can be understood in a noninteracting quasi-particle picture (24–26). In this picture, the dynamics is carried by pairs of initially short-range correlated quasi-particles moving in opposite directions as illustrated in Fig. 1*B*. In all three experimental settings, the autocorrelations remain intact on the diagonal throughout the evolution, due to initially correlated comoving quasi-particle pairs (Fig. 1*B*).

The evolution of the anticorrelation fronts, on the other hand, is determined by the propagation of initially correlated counter-moving quasi-particle pairs and hence propagate away from the diagonal. As illustrated in the space–time sketches of Fig. 1*B*, this demonstrates the spreading of correlations to longer length scales due to the separation of initially correlated quasi-particle pairs. When the density profile is homogeneous, the anticorrelation fronts are consistent with straight lines throughout the dynamics. For the inhomogeneous density profiles the anticorrelation fronts curve up over time which is a key qualitative effect of the quantum-simulated curved metric. Additional effects can arise in finite size systems, due to possible reflections of fluctuations at the boundaries (27).

In cases with sharp boundaries (first two rows of Fig. 1), we observe the formation of perpendicular (antidiagonal) fronts propagating inward from the system boundaries. Unlike the fronts parallel to the diagonal, the perpendicular ones correspond to positive correlations. The sign change is consistent with a reflection of the direction of the current fluctuation at the boundary of the system, i.e., the change in sign of the velocity for quasi-particles scattered at the boundary (see the reflected trajectories in Fig. 1*B*). Note that for reflecting boundaries the perpendicular front spans the entire system (see, e.g., in the homogeneous case at $t = 12$ ms).

The Top Right corner plot of Fig. 1*A* also reveals further insight into the dynamics of the system: The quench dynamics has transformed the initial thermal correlations into a configuration similar to the so-called "rainbow" (28). This term is an intuitive way of designating configurations where correlations are present only between pairs of points symmetric with respect to the middle. A correlation matrix with this X-shaped pattern means that, apart from autocorrelations (diagonal), there are also correlations between pairs of points $(z, L-z)$ on the antidiagonal. Representing correlations between such pairs as noncrossing links connecting them in real space would yield a pattern resembling a rainbow's shape.

In the case with soft boundaries (third row in Fig. 1), no antidiagonal fronts appear, signaling the absence of reflections. This is in accordance with the presence (absence) of reflections for the off-diagonal anticorrelation fronts for sharp (smoothed) edges, presented in Fig. 2. In the presence of sharp edges, the anticorrelation fronts change direction and return to their initial position, resulting in an approximate but clearly visible recurrence of the correlations (c.f. ref. 10). In contrast, for the soft boundary, we observe the slow-down of the anticorrelation fronts and the absence of reflections and recurrences at longer times.

Theoretical Interpretation

The Gaussian field theory in an inhomogeneous metric, i.e. Eq. **1** for $K(z) \equiv K$, allows for an exact geometric explanation of correlation front dynamics. The massless unitary evolution of the velocity field in homogeneous infinite space is a superposition of two local 'chiral' components $\hat{\chi}_\pm$ evaluated at counterpropagating locations

$$\hat{u}(z,t) = \hat{\chi}_+(z+vt) + \hat{\chi}_-(z-vt). \qquad [5]$$

Thus, the time-dependent correlations can be derived by tracing the chiral components $\hat{\chi}_\pm$ from their origin at $t = 0$. The initial correlation length is short, so at $t = 0$ two-point correlations $\langle \hat{\chi}_\sigma(z)\hat{\chi}_{\sigma'}(z')\rangle$ with $\sigma, \sigma' = \pm$ can be significant only for nearby points $z \approx z'$ (c.f. Fig. 1). During the dynamics, this translates to the condition $|z-z'| \approx 2vt$ which corresponds to the positions of the anticorrelation fronts in the experiment. Thus, we expect the anticorrelation front to propagate at twice the sound velocity.

We discuss the conditions for the other fronts and the modification of the above calculation accounting for a finite size system with sharp edges in *SI Appendix*. The sign switching after reflections is consistent with an effective boundary condition of the Neumann type for the phase field, i.e., vanishing of the velocity field at the edges (29). This is the right choice of boundary conditions for an atomic gas trapped in a box-like potential, as the particle current $\hat{j}$ vanishes at the edges.

When tracing the positions in the inhomogeneous case we need to account for the space-dependent sound velocity. To this end, we replace time in the equations describing the positions of the fronts by the actual traveling time for a particle to propagate through a given space interval

$$\tau(z,z') = \int_z^{z'} \frac{\mathrm{d}l}{v(l)}. \qquad [6]$$

The anticorrelation front consists of points z, z' satisfying $|\tau(z,z')| \approx 2t$ which generalizes the condition for the flat metric (See *SI Appendix* for analogous, though more complicated, relations for the reflected fronts). Correlation fronts are therefore curved instead of straight lines.

From the experimental data, we quantify the position dependence of the effective front velocity. We estimate the front location in cuts perpendicular to the diagonal ($z' = -z$)

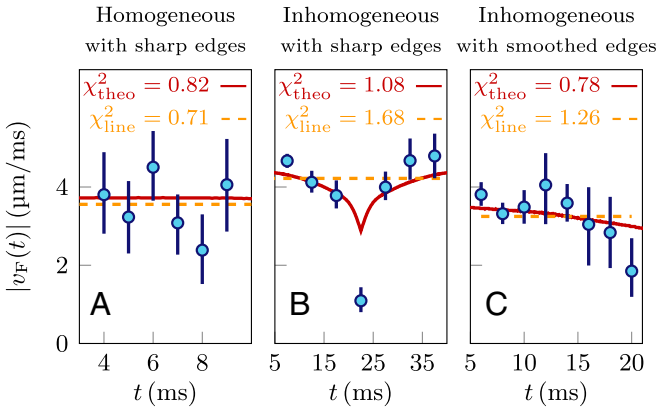

Fig. 3. Estimation of the average front velocity for three settings introduced in Fig. 1. The extracted velocities are shown with blue circles. The error bars show 68% confidence intervals obtained via bootstrapping (30). The red lines represent twice the speed of sound calculated from the experimental local density, $\rho_0(z)$. The orange line is a vertical line marking the average value of the blue circles. The χ^2 is the reduced chi-squared values comparing red/orange curves with the blue circles (for details *SI Appendix*).

at different propagation times t and compute the average front velocity $v_F(t)$ via the difference quotient. In Fig. 3, we compare the measured $v_F(t)$ (blue circles) with the theoretical prediction (red line) and a constant velocity (orange line). In the homogeneous case, the measured front propagation is consistent with a constant velocity (a horizontal line in Fig. 3*A*). For the inhomogeneous density profiles, shown in Fig. 3 *B* and *C*, the effective velocities depend on position in accordance with the theoretically predicted inhomogeneous metric.

The reflection of the correlation front is also clearly visible in Fig. 3*B*, and we find reasonable agreement to the free Gaussian model Eq. **1**. Therein, if the velocity decreases slower than linearly toward the boundary, the traveling time diverges, so there is neither reflection nor turn. Therefore, light-like trajectories converge asymptotically to the boundary, in agreement with the geodesics of Eq. **2**. This is in agreement with experimental observations (Figs. 2 and 3*C*). Note however, that the Tomonaga–Luttinger liquid description is expected to break down near the edges due to vanishingly low atomic density (31) and hence the absence of reflections might be dominated by dispersive or higher-order corrections to the Gaussian model Eq. **1**.

Conclusion

Going beyond previous studies of tunneling-coupled one-dimensional gases (3, 10, 32–35), our results for the velocity field correlations provide a direct measurement of the underlying light-cone propagation. Controlling the local propagation speed of fluctuations $v(z)$, by shaping a stationary inhomogeneous average density, we investigated the propagation of correlation fronts in three distinct settings. In all cases, the experimentally observed light-cone propagation in our quantum field simulator was in good agreement with theoretical predictions for a bosonic Gaussian field theory in the analogue metric $g_{\mu\nu}$ (Eq. **2**). Designing the boundary conditions, we have discussed the presence/absence of recurrences based on the reflection of correlation fronts. Additionally, our measurements reveal that the quench dynamics together with reflections from boundaries transform the initial thermal correlations into the so-called rainbow correlations at half of the recurrence time.

Our work opens the possibility for detailed studies of dynamics and correlations in an inhomogeneous metric. The ability to study the spatially resolved field ϕ together with the high level of control offered by the digital micromirror device, that shapes the spatiotemporal evolution of the averaged background density, offers a versatile platform. In particular, designing $v(z) \sim z^{-\kappa}$ would enable investigation of possible divergence of the signaling time for $\kappa < 1$. This would shed light on the physics close to smoothed boundaries where corrections to Eq. **1** have to be taken into account. Beyond simulating dynamics in curved space–times, the presented quantum field simulator can be used to study dynamics in inhomogeneous $1+1$-dimensional quantum fluids, which have attracted significant theoretical interest (36–50) in general, and the inhomogeneous Tomonaga–Luttinger liquid model with a spatially dependent $K(z)$, in particular, which is theoretically expected to exhibit a breaking of the Huygens–Fresnel principle (51). It is the hope that the present work stimulates such further quantum simulations of curved geometries.

In this work, we study a free noninteracting field theory. However, tuning the strength of the tunneling-coupling between the two superfluids enables us to realize an interacting and even strongly correlated quantum field (8, 9, 35). Whereas the equilibrium properties of this system are well understood and described by the sine–Gordon model, studying the dynamics of its excitations and the resulting information transfer is a theoretical challenge and a future goal of our experiments.

Data, Materials, and Software Availability. The extracted phase profiles for the measurements reported in this work along with an example script calculating the velocity field and its two-point correlation function can be found in ref. 52. Data have been deposited in https://doi.org/10.5281/zenodo.7686404.

ACKNOWLEDGMENTS. We would like to thank B. Rauer, and T. Schweigler for helpful discussions in the early stage of the project. We also thank S. Weinfurtner for fruitful discussion. S. S. would also like to thank P. Moosavi for discussions on theoretical aspects. This work has been supported by the DFG/FWF CRC 1225 'Isoquant', the DFG/FWF Research Unit FOR 2724 'Thermal machines in the quantum world", and the FQXi program on 'Information as fuel' ESQ Discovery Grant 'Emergence of physical laws: from mathematical foundations to applications in many-body physics' of the Austrian Academy of Sciences (OÄW). J.E. has also been supported by the DFG CRC 183 and the BMBF (MUNIQC-ATOMS), as well as by the EU's Horizon 2020 research and innovation program under grant agreement No. 817482 (PASQuanS). M.G. acknowledges support through the start-up grant of the Nanyang Assistant Professorship of Nanyang Technological University, Singapore which was awarded to Nelly Ng. F.C., F.M., and J. Sabino acknowledge support from the Austrian Science Fund (FWF) in the framework of the Doctoral School on Complex Quantum Systems (CoQuS). J. Sabino acknowledges support by the Fundação para a Ciência e Tecnologia, Portugal (PD/BD/128641/2017). G.G. acknowledges support from the European Union's Horizon 2020 research and innovation program under the Marie Skłodowska-Curie grant agreement No. 101026667. S.S. acknowledges support from the European Union's Horizon 2020 research and innovation program under the Marie Skłodowska-Curie grant agreement No. 101030988.

Author affiliations: [a]Vienna Center for Quantum Science and Technology, Atominstitut, TU Wien, Vienna 1020, Austria; [b]School of Physical and Mathematical Sciences, Nanyang Technological University, Singapore 639673, Republic of Singapore; [c]Dahlem Center for Complex Quantum Systems, Freie Universität Berlin, Berlin 14195, Germany; [d]Département de Physique, École Polytechnique, Palaiseau 91120, France; [e]Department of Physics, Instituto Superior Técnico, Universidade de Lisboa, Lisbon 1049-001, Portugal; [f]Institute of Theoretical and Computational Physics, Department of Physics, University of Crete, 71003 Heraklion, Greece; and [g]Helmholtz-Zentrum Berlin für Materialien und Energie, Berlin 14109, Germany

Author contributions: M.T. and P.S. performed the experiment with contributions by F.C., J. Sabino, F.M., and S.-C.J.; M.T., and N.S. analysed the experimental data; M.G., N.S., and S.S. provided the theoretical methodology and calculations with contributions from S.E. and G.G.; J.E. and J. Schmiedmayer provided scientific guidance on experimental and theoretical questions; J. Schmiedmayer conceived the experiment; and All authors contributed to the interpretation of the data and to the writing of the manuscript.

1. M. Peskin, D. Schroeder, *An Introduction to Quantum Field Theory, Frontiers in Physics* (Westview Press, 1995).
2. M. Cheneau *et al*., Light-cone-like spreading of correlations in a quantum many-body system. *Nature* **481**, 484–487 (2012).
3. T. Langen, R. Geiger, M. Kuhnert, B. Rauer, J. Schmiedmayer, Local emergence of thermal correlations in an isolated quantum many-body system. *Nat. Phys.* **9**, 640–643 (2013).
4. J. I. Cirac, P. Zoller, Goals and opportunities in quantum simulation. *Nat. Phys.* **8**, 264 (2012).
5. J. Eisert, M. Friesdorf, C. Gogolin, Quantum many-body systems out of equilibrium. *Nat. Phys.* **11**, 124–130 (2015).
6. B. Yang *et al*., Observation of gauge invariance in a 71-site Bose–Hubbard quantum simulator. *Nature* **587**, 392–396 (2020).
7. Z. Y. Zhou *et al*., Thermalization dynamics of a gauge theory on a quantum simulator. *Science* **377**, 311–314 (2022).
8. T. Schweigler *et al*., Experimental characterization of a quantum many-body system via higher-order correlations. *Nature* **545**, 323 (2017).
9. T. V. Zache, T. Schweigler, S. Erne, J. Schmiedmayer, J. Berges, Extracting the field theory description of a quantum many-body system from experimental data. *Phys. Rev. X* **10**, 011020 (2020).
10. B. Rauer *et al*., Recurrences in an isolated quantum many-body system. *Science* **360**, 307 (2018).
11. M. Gluza *et al*., Mechanisms for the emergence of Gaussian correlations. *Sci. Post Phys.* **12**, 113 (2022).
12. T. Giamarchi, *Quantum Physics in One Dimension* (Clarendon Press, Oxford, 2004).
13. C. Barceló, S. Liberati, M. Visser, Analogue gravity. *Living Rev. Rel.* **14**, 1–159 (2011).
14. M. J. Jacquet, S. Weinfurtner, F. König, The next generation of analogue gravity experiments. *Philos. Trans. R. Soc. A: Math. Phys. Eng. Sci.* **378**, 20190239 (2020).
15. J. R. M. de Nova, K. Golubkov, V. I. Kolobov, J. Steinhauer, Observation of thermal Hawking radiation and its temperature in an analogue black hole. *Nature* **569**, 688–691 (2019).
16. V. I. Kolobov, K. Golubkov, J. R. M. de Nova, J. Steinhauer, Observation of stationary spontaneous Hawking radiation and the time evolution of an analogue black hole. *Nat. Phys.* **17**, 362–367 (2021).
17. J. C. Jaskula *et al*., Acoustic analog to the dynamical Casimir effect in a Bose–Einstein condensate. *Phys. Rev. Lett.* **109**, 220401 (2012).
18. S. Eckel, A. Kumar, T. Jacobson, I. B. Spielman, G. K. Campbell, A rapidly expanding Bose–Einstein condensate: An expanding universe in the lab. *Phys. Rev. X* **8**, 021021 (2018).
19. C. Viermann *et al*., Quantum field simulator for dynamics in curved spacetime. *Nature* **611**, 260–264 (2022), https://doi.org/10.1038/s41586-022-05313-9.
20. M. R. Andrews *et al*., Propagation of sound in a Bose–Einstein condensate. *Phys. Rev. Lett.* **79**, 553–556 (1997).
21. M. Tajik *et al*., Designing arbitrary one-dimensional potentials on an atom chip. *Opt. Exp.* **27**, 33474–33487 (2019).
22. P. Calabrese, J. Cardy, Time dependence of correlation functions following a quantum quench. *Phys. Rev. Lett.* **96**, 136801 (2006).
23. T. Schumm *et al*., Matter-wave interferometry in a double well on an atom chip. *Nat. Phys.* **1**, 57–62 (2005).
24. P. Calabrese, J. Cardy, Time dependence of correlation functions following a quantum quench. *Phys. Rev. Lett.* **96**, 136801 (2006).
25. P. Calabrese, J. Cardy, Quantum quenches in extended systems. *J. Stat. Mech.* **2007**, P06008 (2007).
26. M. Cramer, C. M. Dawson, J. Eisert, T. J. Osborne, Exact relaxation in a class of nonequilibrium quantum lattice systems. *Phys. Rev. Lett.* **100**, 030602 (2008).
27. F. H. L. Essler, M. Fagotti, Quench dynamics and relaxation in isolated integrable quantum spin chains. *J. Stat. Mech.* **2016**, 064002 (2016).
28. G. Ramírez, J. Rodríguez-Laguna, G. Sierra, Entanglement over the rainbow. *J. Stat. Mech.* **2015**, P06002 (2015).
29. S. Patrick, A. Geelmuyden, S. Erne, C. F. Barenghi, S. Weinfurtner, Quantum vortex instability and black hole superradiance. *Phys. Rev. Res.* **4**, 033117 (2022).
30. B. Efron, R. Tibshirani, Bootstrap methods for standard errors, confidence intervals, and other measures of statistical accuracy. *Stat. Sci.* **1**, 54–75 (1986).
31. F. Dalfovo, L. Pitaevskii, S. Stringari, Order parameter at the boundary of a trapped Bose gas. *Phys. Rev. A* **54**, 4213–4217 (1996).
32. R. Geiger, T. Langen, I. E. Mazets, J. Schmiedmayer, Local relaxation and light-cone-like propagation of correlations in a trapped one-dimensional Bose gas. *New J. Phys.* **16**, 053034 (2014).
33. T. Langen *et al*., Experimental observation of a generalized Gibbs ensemble. *Science* **348**, 207–211 (2015).
34. T. Langen, T. Schweigler, E. Demler, J. Schmiedmayer, Double light-cone dynamics establish thermal states in integrable 1D Bose gases. *New J. Phys.* **20**, 023034 (2018).
35. T. Schweigler *et al*., Decay and recurrence of non-Gaussian correlations in a quantum many-body system. *Nat. Phys.* **17**, 559 (2021).
36. N. K. Whitlock, I. Bouchoule, Relative phase fluctuations of two coupled one-dimensional condensates. *Phys. Rev. A* **68**, 053609 (2003).
37. M. A. Cazalilla, Bosonizing one-dimensional cold atomic gases. *J. Phys. B* **37**, S1 (2004).
38. V. Gritsev, A. Polkovnikov, E. Demler, Linear response theory for a pair of coupled one-dimensional condensates of interacting atoms. *Phys. Rev. B* **75**, 174511 (2007).
39. J. Dubail, J. M. Stéphan, J. Viti, P. Calabrese, Conformal field theory for inhomogeneous one-dimensional quantum systems: The example of non-interacting fermi gases. *Sci. Post Phys.* **2**, 002 (2017).
40. J. Dubail, J. M. Stéphan, P. Calabrese, Emergence of curved light-cones in a class of inhomogeneous Luttinger liquids. *Sci. Post Phys.* **3**, 019 (2017).
41. Y. Brun, J. Dubail, The inhomogeneous Gaussian free field, with application to ground state correlations of trapped 1D Bose gases. *Sci. Post Phys.* **4**, 037 (2018).
42. K. Gawędzki, E. Langmann, P. Moosavi, Finite-time universality in nonequilibrium CFT. *J. Stat. Phys.* **172**, 353 (2018).
43. E. Langmann, P. Moosavi, Diffusive heat waves in random conformal field theory. *Phys. Rev. Lett.* **122**, 020201 (2019).
44. P. Moosavi , Inhomogeneous conformal field theory out of equilibrium. *Ann. Henri Poincaré* (2021), https://doi.org/10.1007/s00023-021-01118-0.
45. P. Ruggiero, Y. Brun, J. Dubail, Conformal field theory on top of a breathing one-dimensional gas of hard core bosons. *Sci. Post Phys.* **6**, 051 (2019).
46. S. Murciano, P. Ruggiero, P. Calabrese, Entanglement and relative entropies for low-lying excited states in inhomogeneous one-dimensional quantum systems. *J. Stat. Mech.* **2019**, 034001 (2019).
47. A. Bastianello, J. Dubail, J. M. Stéphan, Entanglement entropies of inhomogeneous Luttinger liquids. *J. Phys. A* **53**, 155001 (2020).
48. P. Ruggiero, P. Calabrese, B. Doyon, J. Dubail, Quantum generalized hydrodynamics. *Phys. Rev. Lett.* **124**, 140603 (2020).
49. M. Gluza *et al*., Quantum read-out for cold atomic quantum simulators. *Commun. Phys.* **3**, 12 (2020).
50. P. Moosavi , Exact Dirac–Bogoliubov–de Gennes dynamics for inhomogeneous quantum liquids. arXiv [Preprint] (2022). http://arxiv.org/abs/2208.14467 (Accessed 28 April 2023).
51. M. Gluza , P. Moosavi , S. Sotiriadis , Breaking of Huygens–Fresnel principle in inhomogeneous Tomonaga–Luttinger liquids. *J. Phys. A* **55**, 054002 (2022).
52. M. Tajik *et al*., Relative phase data to 'experimental observation of curved light-cones in a quantum field simulator'. Zenodo, https://doi.org/10.5281/zenodo.7686404. Deposited 19 September 2022.